A New NMR Method of Fluid Characterization in Reservoir Rocks: Experimental Confirmation and Simulation Results

R. Freedman, SPE, and **S. Lo,** Schlumberger; **M. Flaum,** SPE, and **G.J. Hirasaki,** SPE, Rice U.; **A. Matteson,** SPE, Schlumberger; and **A. Sezginer,** Sensys Instruments

Summary

This paper introduces a new magnetic resonance fluid (MRF) characterization method. The MRF method is based on two key ingredients—a new microscopic constituent viscosity model (CVM) and a new multifluid relaxation model. The CVM provides a link between nuclear magnetic resonance (NMR) relaxation times and molecular diffusion coefficients in hydrocarbon mixtures such as crude oils. The multifluid relaxation model accounts for the T_2 decay of spin-echo signals that arises from intrinsic spin-spin interactions, surface relaxation, and attenuation due to molecular diffusion of fluid molecules in a magnetic field gradient. The MRF method exploits the fact that the molecular diffusion coefficients of brine, oil, and gas molecules typically have values that are well separated from one another. Thus, the diffusion attenuation of a suite of measured NMR signals contains sufficient information to allow differentiation of brine, oil, and gas. The method involves the simultaneous inversion of a suite of spin-echo measurements with the new MRF multifluid relaxation model.

The application of the MRF method to magnetic resonance logging data can provide a detailed formation evaluation. The information provided includes total porosity, bulk volume of irreducible water, brine and hydrocarbon saturation, hydrocarbon-corrected permeability, and oil viscosity.

This paper discusses the theory underlying the CVM and validates the model by testing its predictions on hydrocarbon mixtures including live and dead crude oils. The robustness and accuracy of the multifluid inversion is demonstrated by a Monte Carlo simulation of a model carbonate rock that contains brine, oil, gas, and oil-base mud filtrate (OBMF). The MRF method is applied to suites of spin-echo measurements acquired in the laboratory on partially saturated rocks and shown to provide accurate fluid saturation and oil viscosity estimates.

Since the completion of this work, field test results have shown that the MRF method provides a powerful and unique new formation evaluation tool.

Introduction

It is well known in the industry that oil-bearing reservoirs can be misinterpreted or even missed altogether by conventional resistivity-based interpretation. One difficulty is the fact that many oil-bearing reservoirs exhibit anomalously low values of resistivity, which results in spuriously high water saturation estimates. Other difficulties in the interpretation of resistivity logs can be traced to fresh formation waters or waters with unknown or variable salinity. Problems also occur in formations with complex lithologies for which use of default parameter values (e.g., $m = n = 2$) in Archie's equation can result in totally erroneous water saturation estimates.

The purpose of this paper is to introduce a new state-of-the-art MRF characterization method. The MRF method overcomes the aforementioned problems inherent in resistivity interpretation. It also provides a wealth of formation evaluation information not obtainable by other well logging or laboratory methods.

The MRF method is based on a new multifluid relaxation model. The method relies on the different sensitivities of spin-echo measurements to the fluids present in rock formations when a suite of measurements is acquired with different pulse parameters. In general, a measurement suite consists of spin-echo sequences acquired with different echo spacings, polarization times, applied magnetic field gradients, and numbers of echoes. Such measurements are sensitive to the viscosities and molecular diffusion coefficients of the fluids and therefore provide the information needed for fluid characterization. The inversion of a measurement suite involves a nonlinear fitting of the full data suite to the MRF multifluid relaxation model.

A key ingredient in the multifluid relaxation model is a new microscopic phenomenological model of relaxation and molecular diffusion in liquid hydrocarbon mixtures. This model is referred to as the CVM. It provides an important link between diffusion-free relaxation times and molecular self-diffusion coefficients in crude oils. This link reduces the number of independent parameters needed to characterize the crude oil NMR response and improves the accuracy and robustness of the inversion.

The inversion of a suite of spin-echo measurements using the MRF multifluid relaxation model could be performed without employing the CVM by assuming that the relaxation time and diffusion coefficients are totally independent parameters. This approach, however, involves solving for more unknowns and requires a quantity and quality of data that is not easily obtainable by a moving logging tool. Moreover, to obtain oil viscosity it would still be necessary, following the inversion, to invoke empirical correlations that relate the relaxation times and diffusion coefficients to viscosity. The CVM simplifies the process by using the empirical correlations at the outset to reduce the number of unknowns and directly obtain robust fluid properties from the inversion.

CVM theory predicts that there exist distributions of relaxation times and molecular diffusion coefficients in liquid hydrocarbon mixtures. CVM further predicts that the two distributions are not independent (i.e., if either is known, the other one can be predicted). Moreover, CVM predicts that the mixture viscosity can be estimated from either the relaxation time distribution or the diffusivity distribution and that the two estimates are theoretically equivalent

Scope of the Paper. We present the results of a research and development study that was conducted on three fronts to support the development of the MRF method. The study included the following efforts:

- We conducted Monte Carlo numerical experiments to test the robustness and accuracy of the inversion.
- Laboratory NMR experiments conducted to test the predictions of the CVM consisted of spin-echo and pulse field gradient (PFG) measurements on the following hydrocarbon mixtures

and crude oils: n-hexane-n-hexadecane, n-hexane-squalene, methane-n-hexadecane at seven gas/oil ratios (GORs), four dead crude oils, and a live crude oil at four measured GORs.

- NMR spin-echo measurement suites were acquired on partially and fully saturated Berea 100 and Indiana limestone rock samples. The fluid and rock properties estimated from inversion of the data suites were compared with those estimated by independent laboratory measurements.

This paper elucidates the foundations underlying the MRF method and demonstrates its viability using NMR laboratory measurements and simulation results.

Previous Work. To place the MRF method in perspective, it is prudent to review the currently popular methods of NMR-only fluid characterization.

Published papers on NMR-only fluid characterization applications have for the most part employed the "differential methodology" proposed by Akkurt et al.[1] and Prammer et al.[2] This methodology involves making two or more NMR spin-echo measurements with different wait times. Either the spin-echo measurements or the T_2 distributions computed from them are subtracted to yield a "differential signal" (either a differential T_2 spectrum or spin-echo train) that is further processed to estimate hydrocarbon-filled porosity.

In the literature, the differential methods are referred to either as the differential spectrum method (DSM) or time domain analysis (TDA) method, depending on whether the subtraction is done in the T_2 or time domain.

The TDA method is more robust than the DSM; however, subtracting spin-echo trains leads to a 40% increase in root mean square noise (rmsnoise) on the differential signal. For the differential methods to work, the wait times must be selected so that the differential signal contains negligible contributions from the brine in the formation. To select proper wait times so that the brine contribution is canceled requires knowledge of the NMR properties of the fluids in the formation. This is a limitation of the differential methods for evaluation of exploration wells. Moreover, interpretation of the differential methods requires that the T_1 distribution of the brine phase not overlap with the T_1 spectra of the hydrocarbon phases. This limits the applicability of the differential methods to shaly sands containing very low viscosity oils and gas.

A recent paper by Akkurt et al.[3] noted the limitations of the DSM and TDA methods for oils with low to intermediate viscosities (e.g., 1 to 50 cp). These authors proposed a method called the Enhanced Diffusion Method (EDM) that attempts to exploit the fact that the brine phase is more diffusive than low to intermediate viscosity oils. By increasing the echo spacing so that diffusion dominates the T_2 relaxation of the brine, an upper limit on the apparent brine T_2 can be achieved. Oil-filled porosity is estimated by integrating the apparent T_2 distribution for relaxation times greater than the upper limit.

Although are the basic concept underlying the EDM is valid, there complications in practice that limit its reliability for detection of oil. These include the following: apparent T_2 distributions are broadened by regularization (smoothing) that is applied by the processing; intermediate viscosity crude oils have broad T_2 distributions with short relaxation time tails that overlap the brine T_2 distributions; in exploration well logging it should not be assumed that the diffusivity of the crude oil is less than that of water; and, finally, in wells drilled with oil-base muds it is difficult using the EDM concept to separate the OBMF filtrate signal from that of the native oil.

The MRF method overcomes the fundamental problem associated with the differential methods. That is, the differential methods assume that the brine and hydrocarbon signals can be cleanly separated by subtracting spin-echo measurements (or their associated T_2 distributions) acquired with different pulse parameters. In practice,

crude oils exhibit broad relaxation time distributions; therefore, there will almost always exist some overlap of the oil and brine T_1 distributions, and in some cases there will be total overlap that completely violates the basic premise underlying the differential methods. The MRF method avoids this limitation by the use of a multifluid relaxation model that properly accounts for crude oil and brine T_1 and T_2 distributions even when the two overlap.

The first publication, to our knowledge, to apply a multifluid forward model for NMR fluid characterization is the work of Looyestijn,[4] who used a "diffusion processing" method to compute oil saturations from NMR data acquired using different echo spacings. More recently a more general multifluid relaxation model and inversion method than the model used in Ref. 4 was discussed by Slijkerman et al.[5] These authors discuss a linear forward model and method for determining fluid volumes and relaxation times of different fluid types. The forward model and inversion assume a single relaxation time for the crude oil. This method does not compute the distributions of crude oil relaxation times and self-diffusion coefficients that exist in real crude oils. We show below that the distributions are required to accurately estimate oil viscosity and *BVI*.

Multifluid Relaxation Model

Consider a suite of N spin-echo measurements and let each measurement be characterized by a parameter set $\{W_p, TE_p, G_p, NE_p\}$ for $p = 1,N$ where for the p-th measurement: W_p is the wait time (s), TE_p = the echo spacing (s), G_p = the magnetic field gradient (Gauss/cm) and NE_p = the number of echoes acquired. In practice, the number of different spin-echo measurements composing a suite is a relatively small number (e.g., typically $N \leq 6$). The multifluid relaxation model can be written in the general form

$$A_j^p = \sum_{l=1}^{N_w} a_l \exp\left[-\frac{j * TE_p}{T_{2,l}^\dagger(p)}\right]\left[1 - \exp(-\frac{W_p}{\xi * T_{2,l}})\right] \quad \text{(Brine)}$$

$$+ \sum_{k=1}^{N_o} b_k \exp\left[-\frac{j * TE_p}{T_{2,o}^\dagger(\eta_k, p)}\right]\left[1 - \exp(-\frac{W_p}{T_{1,o}(\eta_k)})\right] \quad \text{(Oil)}$$

$$(1)$$

$$+ A_g \exp\left[-\frac{j * TE_p}{T_{2,g}^\dagger(p)}\right]\left[1 - \exp(-\frac{W_p}{T_{1,g}})\right] \quad \text{(Gas)}$$

$$+ A_{OBMF} \exp\left[-\frac{j * TE_p}{T_{2,OBMF}^\dagger(p)}\right]\left[1 - \exp(-\frac{W_p}{T_{1,OBMF}})\right], \quad \text{(OBMF)}$$

where A_j^p = the amplitude of the j-th echo for the p-th measurement.

The first term in Eq. 1 contains the brine contribution to the signal on the j-th echo. The summation in the first term is over the set of N_w amplitudes $\{a_l\}$ that compose the diffusion-free brine T_2 distribution. The T_{2l} are a set of logarithmically spaced relaxation times owing to bulk and surface relaxation of hydrogen nuclei in the brine. The parameter ξ is an apparent T_1/T_2 ratio for the brine. Note that the polarization functions (i.e., the factors containing W_p) in Eq. 1 are valid for a stationary measurement. For a moving NMR logging tool, speed-dependent polarization functions are used to properly account for speed and magnet prepolarization effects.

The apparent relaxation rate of the brine transverse magnetization including the effects of unrestricted molecular diffusion[6] in the magnetic field gradient is given by

$$\frac{1}{T_{2,l}^{\dagger}(p)} = \frac{1}{T_{2,l}} + \frac{(\gamma_H * G_p * TE_p)^2}{12} D_w(T), \ldots\ldots\ldots(2)$$

$D_w(T)$ is the molecular diffusion coefficient of water molecules[7] at temperature T and $\gamma_H = 2\pi \cdot 4258$ Gauss$^{-1}\cdot$s^{-1} is the proton gyromagnetic ratio. For restricted diffusion, the second term in Eq. 2 is modified.

The second term in Eq. 1 accounts for the signal from the crude oil. The b_k are signal amplitudes from the k-th molecular constituent in the crude oil mixture and $T_{1,o}(\eta_k)$ are longitudinal relaxation times of the constituents. The apparent transverse magnetization relaxation rate of the k-th molecular constituent in the crude oil is given by

$$\frac{1}{T_{2,o}^{\dagger}(\eta_k, p)} = \frac{1}{T_{2,o}(\eta_k)} + \frac{(\gamma_H * G_p * TE_p)^2}{12} D_o(\eta_k), \ldots..(3)$$

where $T_{2,o}(\eta_k)$ is the *diffusion-free* (intrinsic) bulk transverse relaxation time and $D_o(\eta_k)$ is the molecular diffusion coefficient for the k-th molecular constituent in the oil. To simplify the notation, the temperature dependence of $T_{1,o}(\eta_k)$, $T_{2,o}(\eta_k)$, and $D_o(\eta_k)$ is not shown in Eqs. 1 and 3. Note that we have made the assumption that reservoir rock surfaces are preferentially water-wet so that the hydrocarbon relaxation times are not affected by surface relaxation. This assumption is not essential (i.e., the MRF multifluid relaxation model can be modified to handle relaxation in mixed or water-wet rocks). The η_k are phenomenological microscopic parameters referred to as "constituent viscosities" in the CVM. These parameters provide an important link between diffusion-free relaxation times and molecular diffusion coefficients in liquid hydrocarbon mixtures. For live oils containing solution gas, the relaxation times $T_{2,o}(\eta_k)$ and $T_{1,o}(\eta_k)$ have an explicit dependence on GOR. The dependence of $T_{2,o}(\eta_k)$ and $T_{1,o}(\eta_k)$ on η_k and on GOR for live oils is discussed in detail in the section on the CVM.

The third and fourth terms in Eq. 1 represent signals from gas and OBMF, respectively. The relaxation of gas and OBMF signals can be described by single exponential decays with amplitudes A_g and A_{OBMF}, respectively. The OBMF signal in Eq. 1 should be included in the evaluation of formations drilled with oil-base muds. The apparent gas transverse magnetization relaxation rate is

$$\frac{1}{T_{2,g}^{\dagger}(p)} = \frac{1}{T_{2,g}(P,T)} + \frac{(\gamma_H * G_p * TE_p)^2}{12} D_g(P,T), .(4)$$

where $T_{2,g}(P,T) = T_{1,g}(P,T)$ are gas relaxation times and $D_g(P,T)$ is the gas molecular diffusion coefficient. Plots of these quantities as functions of temperature (T) and pressure (P) for methane gas are shown by Kleinberg and Vinegar.[7]

The apparent OBMF transverse relaxation rate is given by

$$\frac{1}{T_{2,OBMF}^{\dagger}(p)} = \frac{1}{T_{2,OBMF}} + \frac{(\gamma_H * G_p * TE_p)^2}{12} D_{OBMF}, \ldots..(5)$$

where $T_{2,OBMF}$ is the diffusion-free transverse relaxation time of the filtrate. It can usually be assumed that the longitudinal and transverse relaxation times are equal (i.e., $T_{2,OBMF} = T_{1,OBMF}$). The OBMF diffusion coefficient D_{OBMF} and relaxation times can be estimated from laboratory measurements of the OBMF viscosity and used as inputs in Eq. 1. If suitable laboratory measurements are not available, then the in-situ OBMF viscosity can be treated as an unknown parameter that is estimated in the inversion of Eq. 1. As noted above, if gas is dissolved in the OBMF, then the OBMF relaxation times have an explicit dependence on GOR. To simplify the notation, the temperature dependence of $T_{1,OBMF}$, $T_{2,OBMF}$, and D_{OBMF} is not shown in the equations above. Eq. 1 assumes that crude oil and OBMF in the flushed zone exist as two separate fluids (i.e., that there is a piston-like displacement of the crude oil by the invading OBMF and that the mixing of the two fluids by diffusion is negligible). If this assumption is not valid, then the two separate fluids can be treated as a mixture in Eq. 1.

Inversion of the Multifluid Relaxation Model. An efficient, fast, accurate, and robust real-time algorithm has been developed to perform the nonlinear inversion of the relaxation model. CPU times for inversion of a typical data suite on a PC Windows machine with a 450-MHz Pentium processor were less than one second. Freedman[8] has published the mathematical details of the inversion algorithm used to obtain the results shown in this paper. To test the inversion, Monte Carlo simulations were performed for model rock formations containing brine, crude oil, gas, and OBMF. The simulations were designed to explore a wide range of fluid and rock properties. The simulation results show that:

- The inversion is robust and accurate over a wide range of hydrocarbon and rock properties.
- Gas can be easily identified because its diffusion coefficient is significantly greater than that of the flushed-zone liquids. The inversion provides accurate estimates of the gas amplitude in Eq. 1 even in the presence of crude oil (for example, in a reservoir where the pressure is below the bubblepoint pressure). The largest source of uncertainty in the estimated gas volumes and saturations results from uncertainties in the gas hydrogen index.
- Crude oil saturations can be quantitatively estimated even in the presence of OBMF and gas, provided that there exists sufficient viscosity contrast between the oil and OBMF. As expected, if the native oil and OBMF have similar relaxation times and diffusion coefficients, then it is not possible to compute accurate saturations; the inversion will confuse the two fluids and cannot differentiate one from the other. In such cases the oil saturation will be overestimated and the OBMF saturation underestimated, or vice versa.
- The inversion is robust and accurate for a wide range of crude oil viscosity. This range is from very low (i.e., of the order of one cp) viscosity to moderately high viscosity on the order of 100 cp. The inversion is more difficult for higher-viscosity oils and is less accurate for oils with viscosity in excess of about 100 cp. This results, in part, from loss of sensitivity to diffusion——the diffusion-induced relaxation rate is negligible compared to the intrinsic (diffusion-free) relaxation rate for high-viscosity oils. Moreover, the relaxation times for high-viscosity oils are comparable to those of the *BVI* so that it is difficult to differentiate high-viscosity oil from *BVI*.
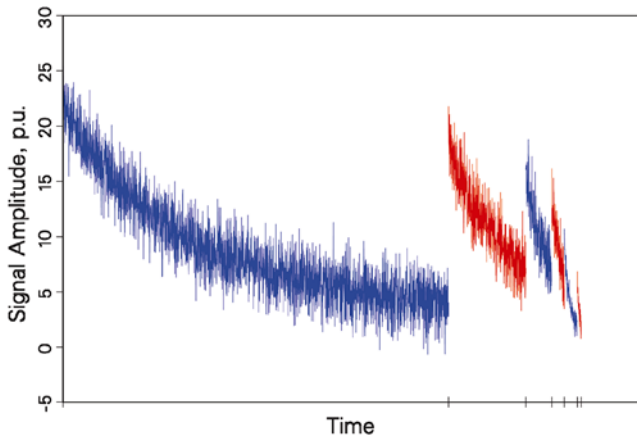
Fig. 1—Synthetic spin-echo measurement suite used for the Monte Carlo simulation of a model carbonate formation containing brine, crude oil, gas, and OBMF. The measurement suite consisted of six phase-corrected Carr-Purcel-Meiboom-Gill (CPMG) spin-echo sequences that have different wait times, echo spacings, magnetic field gradients, and echo numbers. The tick marks on the *x*-axis show the start and finish of echo acqusition for each CPMG. The "time" on the *x*-axis is the echo acquisition time and does not include the wait time that precedes each CPMG. This suite of measurements was used to invert the multifluid relaxation model in Eq. 1. In this simulation, the rmsnoise per echo was equal to 1.8 p.u. for the first two CPMGs and 0.6 p.u. for the other four CPMGs.

Monte Carlo Inversion Results. It is instructive to discuss the results of an inversion of the multifluid relaxation model. The results shown for this example are representative of the results from many other simulations that were performed for a wide variety of fluid and rock properties. Suites of noisy synthetic spin-echo sequences were generated using Eq. 1 for a model formation containing brine, crude oil, gas, and OBMF. This example represents a challenging numerical test of the accuracy and robustness of the MRF inversion. Each data suite consisted of six different spin-echo measurements. It is worth noting that fewer measurements suffice in practice. Freedman et al.[9] have used suites of data with four spin-echo measurements in recent field applications of the MRF method. A typical data suite for one realization of the random noise that was used in the Monte Carlo simulation is shown in Fig. 1. The brine T_2 distribution used for the simulation is shown in Fig. 2. It is similar to the T_2 distributions found in many carbonate rocks. In this example, the OBMF viscosity was assumed known and equal to 2 cp. Fig. 3 compares the results of the Monte Carlo simulation with the input fluid saturations and oil viscosity. Also shown are the standard deviations in the fluid saturation and viscosity estimates. The results shown in Fig. 3 clearly demonstrate that Eq. 1 can be accurately inverted for fluid saturations and oil viscosity even when three hydrocarbon fluids are present. For this example, the number of unknown parameters estimated in the inversion of Eq. 1 is equal to 60 (41 brine amplitudes, 8 crude oil amplitudes, 8 crude oil constituent viscosities, OBMF amplitude, gas amplitude, and apparent brine T_1/T_2 ratio).

The MRF method can be also used to provide robust estimates of diffusion-free brine and oil T_2 distributions; however, this requires an alternative implementation of the inversion algorithm that differs slightly from the one used in this paper. The alternative implementation is discussed in Ref. 8 and is used to process field and laboratory data in Ref. 9.

Monte Carlo simulations like the one discussed in the previous paragraph serve to establish the numerical accuracy and robustness of the MRF inversion for synthetic data. To establish the viability of the MRF method for real fluid-saturated rocks, it is necessary to also show that the relaxation model is based on
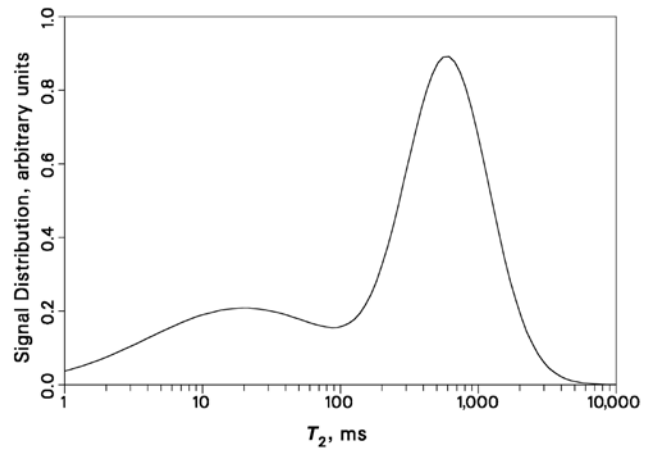

Fig. 2—The brine T_2 distribution used in the carbonate Monte Carlo simulation referred to in Fig. 1.

correct physics. It is therefore necessary to confirm with laboratory experiments that CVM provides an accurate description of NMR relaxation and molecular diffusion in hydrocarbon mixtures and crude oils and that the MRF inversion can be used to accurately estimate fluid saturations and oil viscosities in controlled experiments conducted on partially and fully saturated rock samples. This is discussed in the section entitled Experimental Confirmation.

Formation Evaluation Parameters Estimated From the Inversion of the Multifluid Relaxation Model. The following answer products provided by the MRF method are computed following the inversion of the multifluid relaxation model.

Flushed-Zone Fluid Volumes. The brine-filled porosity, $\phi_{w,xo}$, is computed from the equation

$$\phi_{w,xo} = \frac{1}{HI_w} \sum_{l=1}^{N_w} a_l, \quad \dots\dots\dots\dots\dots\dots\dots\dots\dots\dots\dots\dots\dots\dots(6)$$
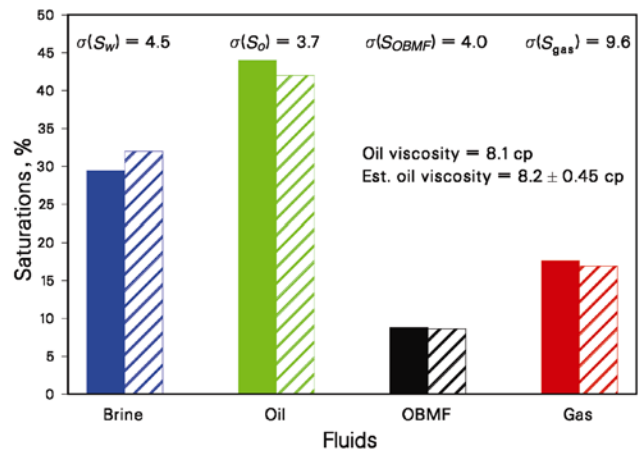
Fig. 3—Comparison of the input fluid properties with the results of a Monte Carlo simulation for a model carbonate formation containing brine, crude oil, gas, and OBMF. The solid bars show the input fluid saturations, and the striped bars show the MRF Monte Carlo estimates. The input and estimated oil viscosities are also shown. Note the accuracy and small standard deviations in the estimates.

where it has been assumed that, except for the hydrogen index correction, the spin-echo amplitudes used in the inversion are in calibrated porosity units. The brine hydrogen index can be estimated from the salinity of the formation water.[7] The a_l are the amplitudes in the brine T_2 distribution. BVI is computed from the equation,

$$BVI = \frac{1}{HI_w} \sum_{l=1}^{N_{cut}} a_l, \quad \dots\dots\dots\dots\dots\dots\dots\dots\dots\dots(7)$$

where the summation is over the N_{cut} brine amplitudes with relaxation times ($T_{2,l}$) less than the bound-water T_2 cut-off ($T_{2,cut}$). The free-water volume, $\phi_{wf,xo}$, is computed from the difference

$$\phi_{wf,xo} = \phi_{w,xo} - BVI, \quad \dots\dots\dots\dots\dots\dots\dots\dots\dots\dots(8)$$

$T_{2,cut}$ can be determined empirically from the maximum observable T_2 after an initially water-saturated rock is centrifuged to remove the free water.[10] Typical values of $T_{2,cut}$ are 33 and 100 ms for sandstone and carbonate rocks, respectively. The flushed-zone oil volume, $\phi_{o,xo}$, is computed from the equation

$$\phi_{o,xo} = \sum_{k=1}^{N_o} \frac{b_k}{HI_{o,k}} \cong \frac{1}{HI_o} \sum_{k=1}^{N_o} b_k, \quad \dots\dots\dots\dots\dots\dots(9)$$

and similarly for the gas and OBMF volumes:

$$\phi_{g,xo} = \frac{A_g}{HI_g}, \quad \dots\dots\dots\dots\dots\dots\dots\dots\dots\dots\dots\dots\dots\dots(10)$$

and

$$\phi_{OBMF,xo} = \frac{A_{OBMF}}{HI_{OBMF}}, \quad \dots\dots\dots\dots\dots\dots\dots\dots\dots\dots\dots\dots (11)$$

In Eq. 9 we have replaced the distribution of hydrogen indices of the molecular constituents in the crude oil by the macroscopic or measured hydrogen index (i.e., $HI_{o,k} \approx HI_o$). The hydrogen indices of dead crude oils can be estimated from the API gravity and are close to one for gravities greater than 25°API.[7] The hydrogen index of OBMF can either be measured using NMR or computed from the known chemical formula, molecular weight, and number of hydrogen nuclei in the chemical formula. Formulas for the hydrogen index of live oils as a function of temperature, pressure, and solution GOR have been published by Zhang *et al.*[11]

Flushed-Zone Fluid Saturations. The flushed-zone fluid saturations are computed from the fluid volumes. For example, the oil saturation $S_{o,xo}$ is computed from the equation,

$$S_{o,xo} = \frac{\phi_{o,xo}}{\phi_{w,xo} + \phi_{o,xo} + \phi_{g,xo} + \phi_{OBMF,xo}} \equiv \frac{\phi_{o,xo}}{\phi_T}, \quad \dots\dots\dots(12)$$

where the total NMR porosity (ϕ_T) has been defined. The other fluid saturations are computed using analogous equations.

Oil Viscosity. The macroscopic (i.e., measured) crude oil viscosity (η_o) can be computed from the logarithmic mean of the crude oil constituent viscosity distribution using the CVM; i.e.,

$$\log(\eta_o) = \sum_{k=1}^{N_o} f_k \log(\eta_k), \quad \dots\dots\dots\dots\dots\dots\dots\dots(13)$$

where f_k and η_k are the proton fraction and the constituent viscosity, respectively, associated with the k-th crude oil molecular constituent. The f_k are defined by

$$f_k = \frac{b_k}{\sum_{n=1}^{N_o} b_n}, \quad \dots\dots\dots\dots\dots\dots\dots\dots\dots\dots\dots\dots(14)$$

Note that the sum of the f_k terms is equal to one. A derivation of Eq. 13 is given in the later section on the CVM.

Hydrocarbon-Corrected Permeability. The MRF method provides a more accurate estimate of BVI (and therefore permeability) in hydrocarbon-bearing zones than was previously possible. BVI is by definition equal to the total bound-water volume. It contains contributions from both capillary and clay-bound waters.

The Timur-Coates (T-C) permeability equation requires BVI as an input; i.e.,

$$K_{TC} = 10^4 \ \phi_T^4 \ (\frac{FFV}{BVI})^2, \quad \dots\dots\dots\dots\dots\dots\dots\dots\dots\dots(15)$$

where ϕ_T is the total porosity in units of p.u./100 and K_{TC} is the permeability in millidarcy (md) units. FFV is the free-fluid volume and includes movable brine and hydrocarbons.

As already noted, the existing NMR fluid-characterization methods cannot accurately separate brine and oil T_2 distributions. Instead, the previous methods compute apparent T_2 distributions that include contributions from both the brine and hydrocarbon signals. Summation of the amplitudes in the apparent T_2 distribution over all relaxation times less than $T_{2,cut}$ produces an estimate of the bound-fluid volume (BFV). In wet zones, $BFV = BVI$; however, in oil-bearing zones, if the oil T_2 distribution has amplitudes with T_2 values less than $T_{2,cut}$, then $BFV > BVI$. This same effect can also occur in gas-bearing zones if the gas signal has a relaxation time less than $T_{2,cut}$. The solid shaded area in **Fig. 4** shows the difference between BFV and BVI in an oil zone. In hydrocarbon-bearing zones, use of BFV in place of BVI in the T-C equation can result in underestimation of permeability. Computations have shown, in some cases of practical interest, that using BFV in Eq. 15 can result in permeability estimates in oil zones that are pessimistic by more than an order of magnitude.
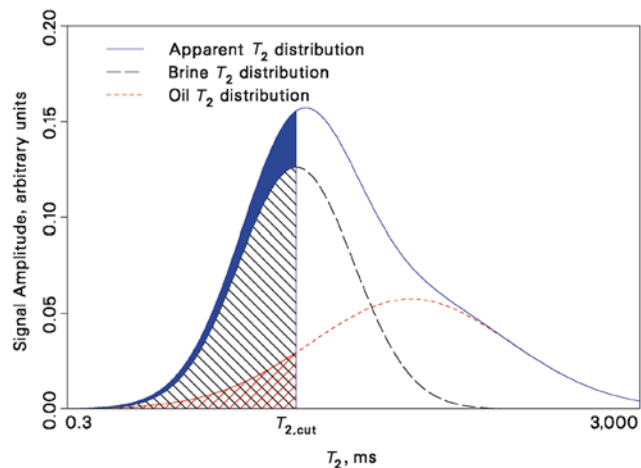
Fig. 4—A schematic showing the difference between *BFV* and *BVI* in an oil zone where the brine and crude oil T_2 distributions overlap. *BFV* and *BVI* are the areas under the apparent and brine T_2 distributions, respectively, that are to the left of $T_{2,cut}$. The solid shaded area shows the difference between *BFV* and *BVI*. The MRF method can separate overlapping crude oil and brine T_2 distributions and therefore can accurately compute the *BVI* required for permeability estimation. Accurate *BVI* estimates are also needed to provide reliable estimates of the potential for water production from oil- and gas-bearing zones.

Constituent Viscosity Model (CVM)

Published experimental NMR and viscosity data for a wide variety of crude oils and other hydrocarbon liquid mixtures[12,13] have shown that their measured viscosities (η_o) are inversely proportional to the logarithmic means ($T_{2,LM}$) of their diffusion-free T_2 distributions. These data can be fit by a macroscopic empirical correlation of the form

$$T_{2,LM} = \frac{aT}{\eta_o(T)}, \quad \text{...................................(16)}$$

where a is an empirically determined constitutive constant and T is the sample temperature in K. The above correlation is for dead hydrocarbon liquids that do not contain solution gas. For live hydrocarbon mixtures and crude oils, the $T_{2,LM}$ have an explicit dependence on GOR,[13] which is discussed below. Since crude oils are mixtures consisting of many different types of hydrocarbon molecules,[14] protons in crude oils do not relax with a single relaxation time. Protons situated on different molecules experience different local fluctuating dipolar fields and therefore relax at different rates, giving rise to a distribution of relaxation times. Typical crude-oil relaxation time distributions consist of a single peak accompanied by a long tail that extends toward shorter relaxation times. The longer relaxation times in the peak are associated with the lighter, smaller molecules in the crude oil, whereas the shorter relaxation times in the tail are associated with the heavier, larger molecules.

One of the missing links in our previous ability to reliably estimate crude oil viscosity from NMR well-log data was the lack of a microscopic physical model for diffusion-free NMR relaxation and molecular diffusion in hydrocarbon mixtures. In special cases, in which the brine and crude oil transverse relaxation time distributions are well separated, accurate estimates of $T_{2,LM}$ from NMR log data are possible, and the viscosity of the crude oil can be reliably predicted using Eq. 16. However, in most situations encountered in practice, the brine and crude-oil distributions overlap, and it has not been previously possible to reliably estimate the $T_{2,LM}$ of the oil distributions from NMR well-log data.

Constituent Viscosities. The CVM makes the hypothesis that the diffusion-free relaxation time $T_{2,k}$ of the k-th molecular constituent in a liquid hydrocarbon mixture is of the same form as the macroscopic empirical viscosity correlation for $T_{2,LM}$; i.e.,

$$T_{2,k} = \frac{aT}{\eta_k(T)}, \quad \text{.......................................(17)}$$

where η_k is the constituent viscosity in centipoise (cp) units. An identical equation can be written for the spin-lattice relaxation time ($T_{1,k}$). For most crude oils, $T_{1,LM} = T_{2,LM}$; however, it has been found that $T_{1,LM} > T_{2,LM}$ for crude oils with high asphaltene content. The η_k are phenomenological molecular variables that have a physical basis similar to the "friction coefficients" used in the Langevin equation treatment of a particle diffusing in a viscous medium.[15]

Recalling the definition of the logarithmic mean, we can write the equation for an n-component mixture

$$T_{2,LM} \equiv T_{2,1}^{f_1} * T_{2,2}^{f_2} * \cdots * T_{2,n}^{f_n}, \quad \text{...................................(18)}$$

where f_k is the proton fraction of the k-th molecular constituent. Combining Eqs. 16, 17, and 18 leads to the result that the macroscopic mixture viscosity is the logarithmic mean of the η_k distribution; i.e., one finds that

$$\eta_o = \eta_1^{f_1} * \eta_2^{f_2} * \cdots * \eta_n^{f_n} \equiv (\eta_k)_{LM}, \quad \text{.........................(19)}$$

which is equivalent to Eq. 13 shown previously. In arriving at the equation above we have used the fact that

$$\sum_{k=1}^{n} f_k = 1, \quad \text{...(20)}$$

Eq. 19 is one of the key results of the CVM and is a "viscosity mixing law" for hydrocarbon mixtures. An important point to emphasize is that the η_k are not the viscosities of the pure mixture constituents—they differ from the latter because of intermolecular interactions in the mixture.

Diffusion Coefficient Distributions. The CVM also makes the hypothesis that in hydrocarbon mixtures and crude oils there exists a distribution of molecular diffusion coefficients of the form

$$D_k = \frac{bT}{\eta_k(T)}, \quad \text{...(21)}$$

where b is an empirical constitutive constant that has been determined from Stejskal and Tanner[13,16] PFG diffusion measurements. D_k is the molecular diffusion coefficient of the k-th constitutent in the mixture. The D_k are not the diffusion coefficients of the pure mixture components because, like $T_{2,k}$, they are modified by intermolecular interactions in the mixture. An equation analogous to Eq. 18 can be written for D_{LM}. Note that the mixture diffusion coefficients in Eq. 21 have the same dependence on T/η_k as that of the diffusion coefficients for pure liquids derived by Einstein in his pioneering theoretical study of Brownian motion.[15]

In the CVM, each hydrocarbon molecule in the mixture is assumed to relax and diffuse as it would in its pure-state liquid, except that the microscopic constituent viscosity replaces the macroscopic pure-state viscosity. The microscopic mixture details such as molecular composition, molecular interactions, and molecular sizes are contained solely in the constituent viscosities that can be determined from NMR measurements.

The constitutive constant a in Eqs. 16 and 17 has been found for a wide variety of crude oils measured at 2 MHz to be well approximated by the value $a = 0.004$ s·cp·K^{-1}, which is used in this paper for all crude oil computations. For pure n-alkanes and methane-n-alkane mixtures, Lo[13] found a larger value, $a = 0.009558$ s·cp·K^{-1}. We believe that the larger value of a found for the pure alkanes and the methane-alkane mixtures is caused by the absence of the short relaxation time tail that is present in crude oil relaxation-time distributions. The constitutive constant b in Eq. 21 has been found to be well approximated by the value $b = 5.05 \cdot 10^{-8}$ cm^2·s^{-1}·cp·K^{-1} for dead and live hydrocarbon mixtures and crude oils. This value is used for the diffusion computations in this paper.

Predictions of the CVM. In addition to Eq. 19, CVM theory leads to several new theoretical predictions that have been confirmed by laboratory experiments. On substitution of Eqs. 17 and 21 into 19, we find that

$$\eta_o = \frac{aT}{T_{2,LM}} = \frac{bT}{D_{LM}} \equiv (\eta_k)_{LM}, \quad \text{...............................(22)}$$

where D_{LM} is the logarithmic mean of the diffusion coefficient distribution. Eq. 22 predicts that the viscosity of a liquid phase hydrocarbon mixture or crude oil can be computed from either the logarithmic mean of the T_2 or the D distribution. The first equality in Eq. 22 is consistent with present-day knowledge (e.g., Eq. 16), whereas the second equality is new. Moreover, the two methods

of computing η_o are theoretically equivalent, and both methods are also equivalent to computing η_o from Eq. 19.

CVM theory also predicts that the ratios of mixture constituent diffusion coefficients to constituent relaxation times are constant. Division of Eq. 21 by 17 leads to

$$\frac{D_k}{T_{2,k}} = \frac{b}{a} = \frac{D_{LM}}{T_{2,LM}} , \dots\dots\dots\dots\dots\dots\dots(23)$$

where the second equality in Eq. 23 follows from Eq. 22.

A consequence of Eq. 23 is that T_2 and D distributions for hydrocarbon mixtures and crude oils are not independent (i.e., if one is known, the other can be computed).

Extension of CVM to Live Hydrocarbon Mixtures and Crude Oils. The CVM can be extended to live hydrocarbon mixtures with existing macroscopic empirical correlations that relate $T_{1,LM}$ and D_{LM} to η_o/T and GOR. In this section we first review these correlations and then discuss the modified CVM equations.

Macroscopic Correlations for Live Hydrocarbon Mixtures. The existing macroscopic empirical correlations for live hydrocarbon mixtures were established using NMR inversion recovery ($T_{1,LM}$) and PFG (D_{LM}) measurements acquired on binary mixtures of methane-n-hexane, methane-n-decane, and methane-n-hexadecane.[13,17] The mixture data were acquired for a wide range of temperatures and pressures with the liquid and vapor phases in thermodynamic equilibrium. This range of temperatures and pressures corresponds to a wide range of GOR. Diffusion-free measurements of $T_{2,LM}$ [e.g., using Carr-Purcell-Meiboom-Gill (CPMG) spin-echo sequences] were not possible in these mixtures because of large diffusion effects on the methane signal in the inhomogeneous field of the NMR spectrometer.

Analysis of the liquid phase methane-n-alkane mixtures data led to the following empirical macroscopic live oil correlations for $T_{1,LM}$ and D_{LM},

$$T_{1,LM} = T_{2,LM} = \frac{a\ T}{\eta_o f(\text{GOR})}, \dots\dots\dots\dots\dots\dots(24)$$

where GOR is defined here as cubic meters of solution gas per cubic meters of stock tank liquid (m^3/m^3) at standard conditions. Standard conditions of temperature and pressure are 60°F and one atmosphere, respectively. GOR can be converted from units of m^3/m^3 to units of cubic feet of gas per barrel of stock tank liquid (ft^3/bbl) at standard conditions by multiplying by a conversion factor equal to 5.62. The empirically determined function f(GOR) in Eq. 24 is given by

$$f(\text{GOR}) = 10^{10^{\alpha}} , \dots\dots\dots\dots\dots\dots\dots\dots(25)$$

where

$$\begin{aligned} \alpha = &-0.127 \left[\log_{10}(\text{GOR}) \right]^2 \\ &+ 1.25 \log_{10}(\text{GOR}) - 2.80 \end{aligned}, \dots\dots\dots\dots\dots\dots(26)$$

The macroscopic empirical correlation for live hydrocarbon mixtures that relates D_{LM} to the mixture viscosity has the same form as the one for dead mixtures; i.e.,

$$D_{LM} = \frac{bT}{\eta_o}, \dots\dots\dots\dots\dots\dots\dots\dots\dots\dots\dots(27)$$

In Eq. 24 we have used the fact that $T_{1,LM} = T_{2,LM}$, because it has been shown for methane-n-alkane mixtures[13] that the fast motion limit $\omega_o \tau_c \ll 1$ is satisfied for the 90-MHz Larmor frequency used in the experiments. In the inequality, τ_c is a typical rotational diffusion correlation time in the mixture that for low viscosity fluids is on the order of 10^{-12} to 10^{-14} seconds, and ω_o is the Larmor angular frequency. In a crude oil, there is a broad distribution of correlation times. We have experimental data that suggest that the correlation times associated with the larger molecules in a crude oil are so long that the fast diffusion condition breaks down at 90 MHz and the equality $T_{1,LM} = T_{2,LM}$ is no longer valid. This is discussed in more detail in the section on live crude-oil measurements.

Examination of Eq. 24 shows that the NMR relaxation times have an explicit dependence on GOR. Of course, both the relaxation times and the diffusion coefficients have an implicit dependence on GOR because the effect of solution gas is to reduce the mixture viscosity. The latter effect tends to increase the relaxation times and diffusion coefficients for live hydrocarbon mixtures and crude oils, whereas the effect of f(GOR) is to reduce the relaxation times because $f(\text{GOR}) \geq 1$.

Modified CVM Equations for Live Mixtures and Crude Oils. Employing the empirical macroscopic correlation in Eq. 24 that was established for methane-n-alkane mixtures, the CVM postulates that

$$T_{2,k} = \frac{aT}{\eta_k f(\text{GOR})}, \dots\dots\dots\dots\dots\dots\dots\dots(28)$$

which is the generalization to live hydrocarbon mixtures of Eq. 17 that is valid for dead hydrocarbon mixtures and crude oils. It is easy to show using Eqs. 18, 24, and 28 that Eq. 19 for the mixture viscosity as a function of the constituent viscosities is also valid for live mixtures. It further follows from Eqs. 24 and 27 that

$$\eta_o = \frac{aT}{T_{2,LM} f(\text{GOR})} = \frac{bT}{D_{LM}} \equiv (\eta_k)_{LM}, \dots\dots\dots\dots(29)$$

The correlation in Eq. 27 says that the CVM constitutive equation (i.e., Eq. 21) for dead mixtures is also valid for live mixtures. Therefore, using Eqs. 21 and 28 shows that the ratio of D_k to $T_{2,k}$ for live hydrocarbon mixtures is given by

$$\frac{D_k}{T_{2,k}} = \frac{b\ f(\text{GOR})}{a} = \frac{D_{LM}}{T_{2,LM}}, \dots\dots\dots\dots\dots\dots(30)$$

Experimental Confirmation

The first part of this section compares the CVM with experimental results for dead and live hydrocarbon mixtures and crude oils. These results confirm the validity of the CVM for hydrocarbon mixtures. The second part of this section compares water saturations estimated from MRF inversions of NMR data suites acquired on partially and fully saturated reservoir rocks with independent estimates of the water saturations. The oil viscosities estimated from the inversions are compared with the known viscosity of the oil in the rock samples.

Comparison of CVM Predictions with NMR and Viscosity Measurements for Two-Component Mixtures. Pulsed field gradient (PFG) and CPMG spin-echo measurements were conducted at 2 MHz on deoxygenated binary hydrocarbon mixtures. These included mixtures with two different molecular compositions: n-hexane-n-hexadecane (C6-C16) and n-hexane-squalene (C6-C30). The room temperature viscosities of pure C6, C16, and C30 are approximately 0.3, 3, and 11 cp, respectively. For each mixture, measurements were made at three different concentrations (i.e., weight fractions) of the constituents. Sample temperatures were held constant at 30°C for all measurements.
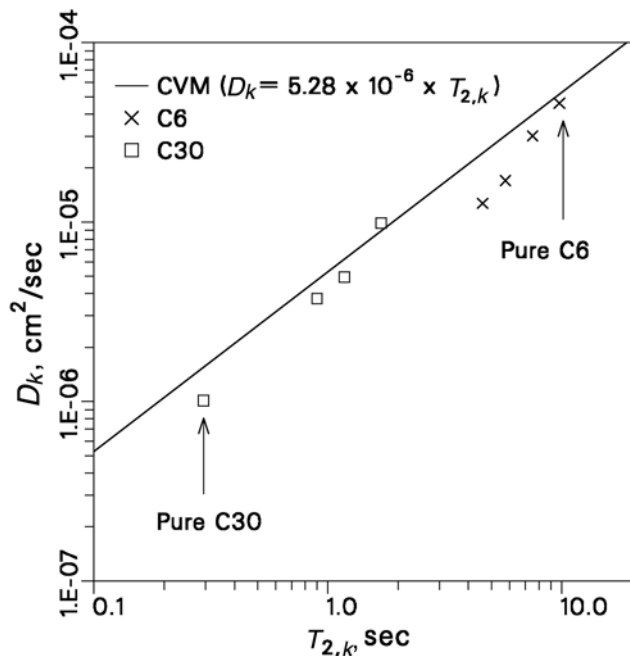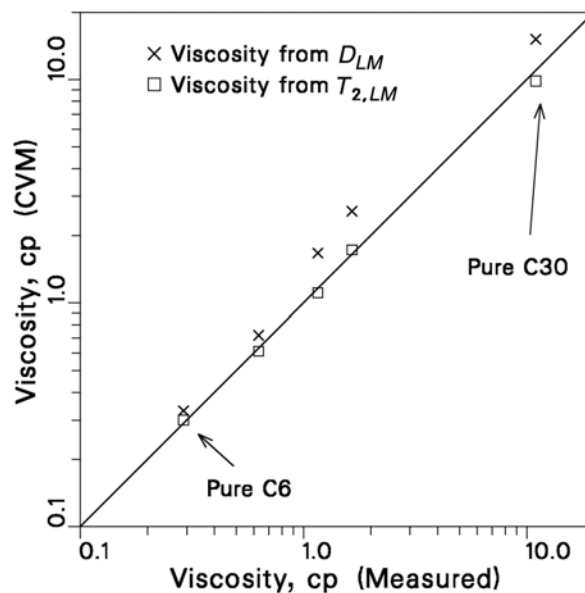
Fig. 5—A plot of NMR measurements of D_k vs. $T_{2,k}$ for n-hexane-squalene mixtures at three concentrations. Also shown are the measured pure component endpoints. The straight line is the relationship predicted by Eq. 23 of the CVM for dead hydrocarbon mixtures.

Fig. 6—A plot of measured vs. CVM-estimated viscosities for n-hexane-squalene mixtures at three concentrations. Also shown are the measured and estimated pure component viscosities. The average absolute percent deviations of the CVM-estimated viscosities from the measured viscosities are 33.1 and 5.2% as computed from D_{LM} and $T_{2,LM}$, respectively.

Diffusion-free relaxation times, $T_{2,k}$, and proton fractions, f_k, of the two mixture constituents were estimated for each mixture concentration by fitting the observed CPMG decays to a four-parameter, two-exponential model. As expected, the proton fractions estimated from the fits agreed very well with the known proton fractions in each sample. These estimates were used in Eq. 18 to compute $T_{2,LM}$ for each mixture. The spin-echo data were acquired using a 2.4-ms echo spacing, and 16,000 echoes were collected so that the long relaxation times of the mixture constituents could be resolved by inversion of the data. Inversion recovery measurements were also conducted on pure C6 to determine its T_1 relaxation time. The good agreement between T_1 from the inversion recovery and T_2 estimated from a CPMG proved that diffusion effects were not present in the CPMG decays, thus demonstrating that the $T_{2,k}$ were free of diffusion effects.

Diffusion coefficients, D_k, and proton fractions, f_k, of the two mixture constituents were estimated for each mixture concentration by fitting a sequence of Stejskal-Tanner[16] PFG spin-echoes to a two-exponential relaxation model. These estimates were used to compute D_{LM} for each mixture.

Fig. 5 shows a log-log plot of the measured D_k vs. $T_{2,k}$ for the C6-C30 mixtures at the three concentrations shown in the figure, plus the pure component endpoints. Also shown on the plot is the CVM-predicted (see Eq. 23) straight line with slope one and intercept b/a. Note that the measured data points fall along the line predicted by the CVM. **Fig. 6** shows good agreement between the measured C6-C30 mixture viscosities for the three different mixture concentrations and those predicted by the CVM using Eqs. 22. Theoretically, according to the CVM, the viscosity estimates obtained from $T_{2,LM}$ and D_{LM} should be equal. The minor differences seen in Fig. 6 result from model and measurement errors. Results similar to those shown in Figs. 5 and 6 were also found for the C6-C16 mixtures and therefore, to save space, will not be shown here.

Comparison of CVM Predictions with NMR and Viscosity Measurements for Dead Crude Oils. Crude oils are complex mixtures that in practice have unknown and highly variable molecular compositions.[14] One of the attractive features of the CVM is that the molecular composition and other details such as molecular sizes and molecular interactions are contained in the η_k distributions that are estimated by inversion of NMR laboratory or well-logging measurements. Both CPMG and PFG measurements were performed at 2 MHz on four crude oils from the Rice U. database to test and compare the viscosity estimators in Eq. 22. We also applied the CVM estimator of crude oil viscosity based on $T_{2,LM}$ to published Belridge field crude-oil data acquired at 2 MHz.[12] PFG data were not available for the Belridge crudes, so the D_{LM} viscosity estimator could not be tested for these oils. **Fig. 7** shows a comparison of CVM-estimated viscosity vs. measured viscosity for 31 Belridge crude oils and the four crude oils from the Rice U. database. The dead oil measurements were made at 25 and 30°C for the Belridge and Rice oils, respectively.

CVM predicts that T_2 and D distributions for hydrocarbon mixtures are not independent—if either is known, the other one can be estimated using Eq. 23 for dead mixtures or Eq. 30 for live mixtures. Measured T_2 and D distributions were determined from CPMG and PFG measurements. To test the CVM prediction, D distributions were computed from the measured T_2 distributions and compared with the measured D distributions.

Fig. 8 compares the measured and computed D distributions for the four Rice U. crude oils. Clearly, the peak positions and general shape of the measured and computed distributions are similar as predicted. However, the measured D distributions from the PFG experiments are missing the very small diffusion coefficients that are seen in the D distributions computed from the CPMG measurements. Because the echo spacings used in the PFG Experiments were in the range from 60 to 80 ms, the signals from very small diffusion coefficients (that correspond to very short relaxation times) were not recoverable.
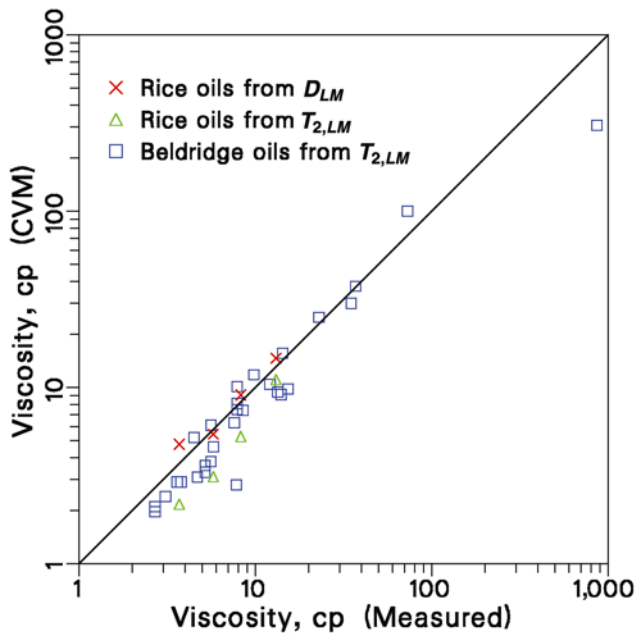
Fig. 7—A plot of measured vs. CVM-estimated viscosities for 31 Belridge field dead crude oils and 4 Rice U. dead crude oils. The average absolute percent deviations of the CVM-estimated viscosities from the measured viscosities are 11.9 and 26.8% as computed from D_{LM} and $T_{2,LM}$, respectively.
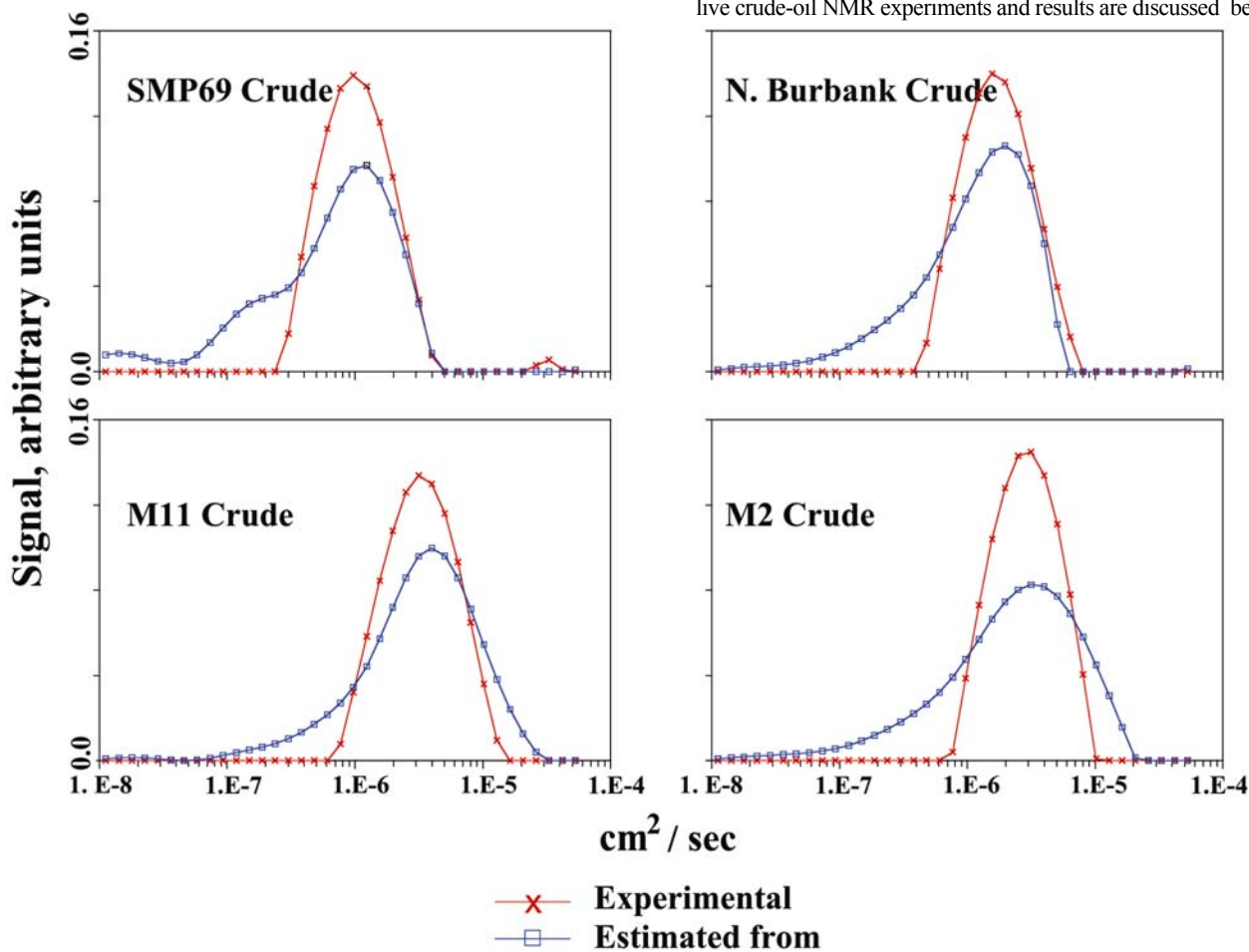
From Eq. 30 the ratio of b/a determines the y-intercept of the line predicted by CVM on a log-log plot of D_k vs. $T_{2,k} \cdot f(\text{GOR})$. **Fig. 9** compares the theoretical CVM line with experimental measurements at seven different GORs. The GORs used in these computations were estimated from measured Rice U. GOR data for methane-n-hexadecane mixtures. The live mixture data fall along the line predicted by CVM. **Fig. 10** shows the comparison of mixture viscosities estimated from CVM with those computed using SuperTrapp, an interactive computer database for the prediction of transport and equilibrium properties of pure hydrocarbons and hydrocarbon mixtures.[18] The reason that there are fewer data points for $T_{2,LM}$ than for D_{LM} is that it was not possible to resolve two distinct components in the C1-C16 relaxation time distributions for all of the GORs used in the experiments.

Comparison of CVM With Live Crude-Oil Measurements. Measurements of viscosity and GOR were made on a live North Sea crude oil in equilibrium with methane gas at 35°C for four saturating bubblepoint pressures, e.g., 1,800, 2,800, 3,500, and 4,000 psia. The measured viscosity and API gravity of the dead oil at room temperature are 9.2 cp and 29.7°API, respectively. The live oil viscosity and GOR measurements were made by a Schlumberger company specializing in laboratory pressure/volume/temperature (PVT) and flow-assurance measurements and are shown in **Table 1.** Note that although the GORs are relatively low, the live oil viscosities are significantly reduced compared to those of the dead oil.

NMR relaxation time and diffusion measurements at 35°C were also made on the live crude oil at the four bubblepoint pressures. The live crude-oil NMR experiments and results are discussed below.

Fig. 8—A comparison, for four Rice U. crude oils, of D distributions measured by PFG measurements with D distributions computed from the measured T_2 distributions using CVM Eq. 23

TABLE 1—MEASURED GOR AND VISCOSITY OF LIVE NORTH SEA CRUDE OIL AT 35ºC		
P (psia)	GOR (m³/m³)	η (cp)
14.7	0	8.89
1,800	45.5	3.64
2,800	70.8	2.74
3,500	88.4	2.26
4,000	101.7	2.14

TABLE 2—MEASURED D_{LM} AND $T_{2,LM}$ OF LIVE NORTH SEA CRUDE OIL AT 35ºC		
GOR (m³/m³)	D_{LM} (cm²/s)	$T_{2,LM}$ (s)
0	1.88×10^{-6}	0.193
45.5	4.37×10^{-6}	0.321
70.8	5.61×10^{-6}	0.388
88.4	6.20×10^{-6}	0.435
101.7	6.42×10^{-6}	0.468

Live Crude-Oil PFG Measurements. Stejskal-Tanner PFG measurements at 30°C of diffusion coefficient distributions were first made at 2 and 90 MHz on the dead crude oil. As we expected, the D distributions were very similar and did not show a frequency dependence. The logarithmic mean diffusion coefficients for the dead oil were almost identical; i.e., $D_{LM} = 1.55 \cdot 10^{-6}$ cm²/s at 2 MHz and $1.48 \cdot 10^{-6}$ cm²/s at 90 MHz. After it was shown that the crude oil D distributions were independent of frequency, the live oil PFG were performed at 90 MHz and 35°C. The D_{LM} data measured on the live crude oil are shown in Table 2. Fig. 11 shows excellent agreement between the CVM viscosities computed using Eq. 27 and the measured viscosities. The data point at 0.3 cp represents a live oil sample with a GOR of 2,200 SCF/bbl (391 m³/m³) at reservoir conditions. Both viscosity and NMR relaxation time data were measured on this live oil by Appel *et al.*[19] Note the excellent agreement between the viscosity estimated using CVM Eq. 24 and the measured viscosity.

Live Crude-Oil Relaxation Time Measurements. Inversion recovery measurements of T_1 distributions at 30°C were first made on the dead crude oil at 2 and 90 MHz. The dead oil T_1 measurements showed a strong frequency dependence (i.e., $T_{1,LM}$ = 176 ms at 2 MHz and 369 ms at 90 MHz). Thus, the T_1 relaxation rate is slower at 90 MHz than at 2 MHz. The T_1 distribution measured at 90 MHz showed an obvious shift toward longer relaxation times compared to the one at 2 MHz. The frequency dependence of T_1 for an intermediate viscosity oil is not surprising because, as noted previously, the fast motion condition, $\omega_o \tau_c << 1$, is not necessarily satisfied for some of the

larger molecules in the crude oil. T_1 measurements were also made at 35°C on the dead and live crude oil at 90 MHz. CPMG measurements of T_2 distributions at 30°C were first made on the dead crude oil at 2 MHz and 90 MHz. The $T_{2,LM}$ of the dead crude oil at 2 and 90 MHz were nearly identical (i.e., $T_{2,LM}$ = 184 ms at 2 MHz and 185 ms at 90 MHz); however, the shortest relaxation times in the 90-MHz T_2 distribution were shifted to the right, and the longest times were shifted to the left compared to those at 2 MHz. Aside from this "squeezing effect" on the 90-MHz T_2 distribution, the frequency dependence of T_2 is much weaker than that of T_1. The measured $T_{2,LM}$ of the dead and live crude oil at 90 MHz and 35°C are shown in **Table 2**. **Fig. 11** shows good agreement between the CVM viscosities computed with CVM Eqs. 24 through 26 and the measured viscosities. The 90-MHz live oil T_2 measurements were made with two echo spacings: 3 and 4 ms. These measurements showed no dependence on the echo spacing, thus proving that the measured T_2 distributions were free of diffusion effects.

Estimation of Water Saturation and Oil Viscosity in Rocks by Inversion of Laboratory NMR Data. The MRF inversion was tested with suites of CPMG spin-echo data acquired at 2 MHz. The data suites were acquired on Berea 100 sandstone (SS) and Indiana limestone (LS) rock samples at 27°C. The samples were cylindrical cores (3.75-cm long and 2.0-cm diameter) that were either fully brine saturated or partially saturated with 0.2 ohm-m brine and S6 oil. S6 oil is a Cannon viscosity standard with a
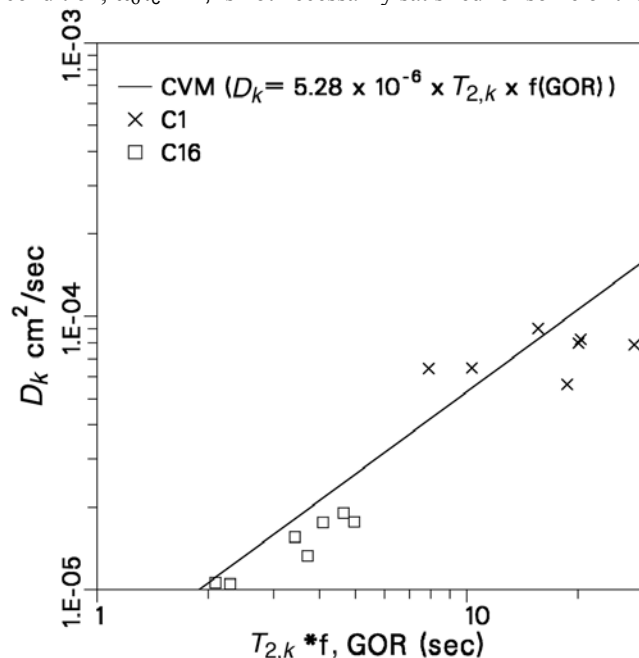
Fig. 9—A plot of NMR measurements of D_k vs. $T_{2,k}$ for methane-n-hexadecane mixtures at seven GORs. The straight line is the relationship predicted by Eq. 30 of the CVM for live hydrocarbon mixtures.
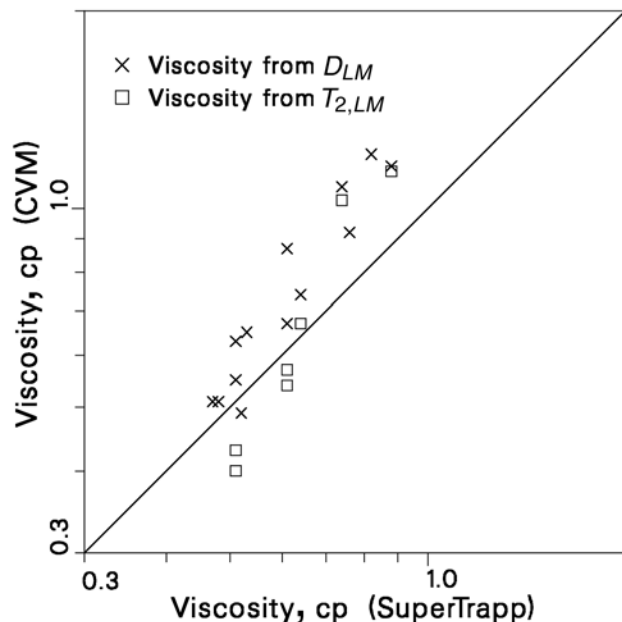
Fig. 10—A plot of CVM-estimated viscosities vs. those computed using SuperTrapp for methane-n-hexadecane mixtures at different GORs. The average absolute percent deviations of the CVM-estimated viscosities from the SuperTrapp viscosities are 22.2 and 18.4% as computed from D_{LM} and $T_{2,LM}$, respectively.
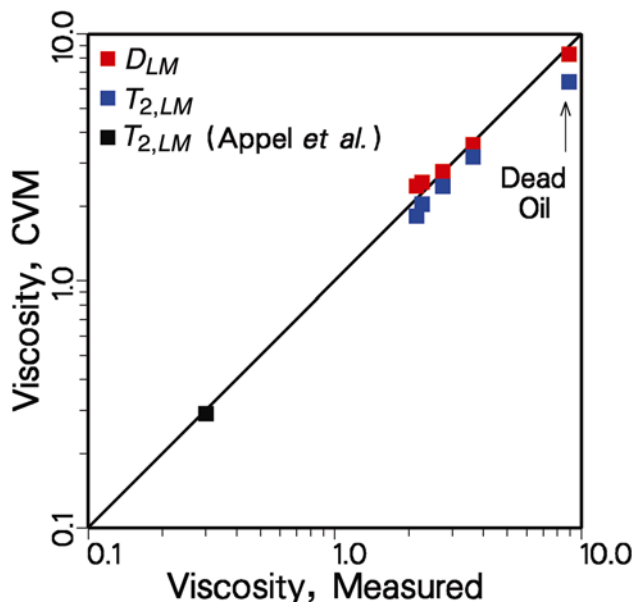
Fig. 11—A plot of measured vs. CVM-estimated viscosities for the live North Sea crude oil, the properties of which are shown in Table 1. The CVM viscosity estimates were computed from Eqs. 24 through 27 and the data in Tables 1 and 2. The average absolute percent deviations of the CVM-estimated viscosities from the measured viscosities are 6.9 and 15.4% as computed from D_{LM} and $T_{2,LM}$, respectively. The data point at 0.3 cp is a live oil, the NMR relaxation time distribution and viscosity of which were measured by Appel et al.[19]

viscosity of 7.5 cp at 27°C. S6 oil has a narrow T_2 distribution centered at approximately 265 ms. The oil distribution is contained within the brine T_2 distributions of both rocks. This complete overlap of the brine and oil distributions would make it difficult even to detect the presence of oil with previous methods.

Five rocks—four Berea 100 and one Indiana limestone—were used in the experiments. For Berea 100 Rocks 3 and 4 and Indiana limestone Rock 5, NMR measurements were conducted with the rocks in fully and partially brine-saturated states. For Berea 100 Rocks 1 and 2, NMR measurements were conducted only for the partially saturated states. Thus, a total of eight suites of CPMG measurements corresponding to the eight different sample saturation states were acquired and processed using the MRF inversion. The experiments were conducted at Schlumberger-Doll Research (SDR). For objective assessment of the results, the eight unlabeled data suites were sent to the Schlumberger Sugar Land Product Center for processing.

The measurement suite for all samples consisted of six CPMGs acquired with different numbers of echoes, echo spacings, and wait times. The data were repeated and averaged until the rmsnoise per echo was equal to 1 p.u. for each CPMG in the suite. **Fig. 12** shows the full suite of R and X-channel CPMGs for partially saturated Berea 100 Rock 3B.

Experimental Procedure. The CPMG data suites were acquired with a commercial 2-MHz NMR spectrometer that was equipped with gradient coils so that a constant magnetic field gradient could be applied to the samples. The static magnetic field of the spectrometer and the gradient field were both applied along the z-axis of the cylindrical rock samples. A constant field gradient, G = 25 Gauss/cm, was used for all measurements. The gradient field produced a 1.6-mm thick resonant slice transverse to the z-axis of the sample.

The five rocks were fully brine saturated and weighed, and their buoyancy porosities were measured. As noted above, NMR measurements were conducted on Rocks 3, 4, and 5 in the fully brine-saturated state. Rocks 3 and 5 were then partially saturated with S6 oil in a centrifuge tube using the following water-drainage
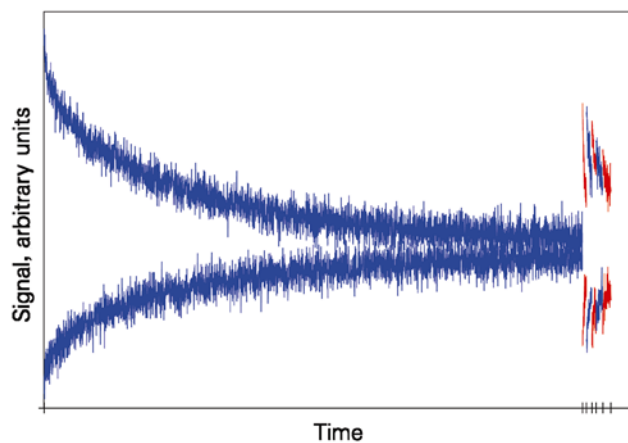

Fig. 12—The measurement suite for the partially saturated Berea 100 Rock 3B shown in Table 3. The R and X-channel spin-echo signals are shown for each of the six measurements in the suite. The rmsnoise per echo on each CPMG is equal to 1.0 p.u. The tick marks on the *x*-axis show the start and finish of echo acquisition for each CPMG. The "time" on the *x*-axis is the echo acquisition time and does not include the wait time that precedes each CPMG

procedure. The rocks were placed in the centrifuge tube on a bed of glass beads and immersed in S6 oil. The rocks were then spun at 3,400 rpm for one hour. After centrifuging, the partially oil-saturated rocks were weighed. The water saturation of each partially saturated rock was estimated using the difference in weight of the fully and partially saturated rock and the known buoyancy porosity, sample volume, and oil and brine mass densities. In weighing the partially saturated rocks, it is necessary to be careful and consistent when dealing with the surface layer of oil. Our procedure was to remove the surface layer of oil using an oil-saturated paper towel.

It should also be noted that the water saturation estimated by the differential weight method (DWM) represents the average saturation in the sample, which can differ from the saturation in a small volume of the sample (e.g., in the 1.6-mm thick resonant volume measured by the NMR). Similarly, the buoyancy porosity is an average porosity that can differ from the NMR porosity because of porosity fluctuations in the sample. For Rocks 1 and 2, the final partial saturation states were not obtained by water drainage in the centrifuge. The final state of saturation for Rock 1 was obtained by imbibition of water. For Rocks 2 and 4, oil was pumped under pressure into the rock in an attempt to achieve irreducible water saturation. The volume of oil pumped into the rock was measured. Problems were encountered with accurately measuring the volume of oil pumped into the sample.

Results of Blind Tests on Rock Samples. **Table 3** shows the results of the blind tests. The NMR-derived water saturations are in good overall agreement with those estimated from laboratory measurements. The average absolute deviation of the CVM-estimated water saturations from the DWM-estimated water saturations is 7.7%. The largest difference between the NMR and laboratory water saturation estimates is for Rock 2B. For this sample, the estimated volume of oil pumped into the sample is too high, leading to an estimated water saturation that is obviously too low (i.e., it is below the irreducible water saturation for Berea 100). The NMR-derived viscosities in Table 3 are also in good agreement with the 7.5 cp viscosity of the S6 oil. The largest viscosity error is for Rock 1B. This is the only sample for which the final saturation state was achieved by water imbibition instead of water drainage. We believe that the NMR overestimation of the oil viscosity in Rock 1B might be related to "restricted diffusion" of the oil in this sample because of the presence of an emulsion of water droplets and oil produced by the water imbibition. Note that

TABLE 3—NMR VS. LAB MEASUREMENTS ON PARTIALLY SATURATED ROCKS AT 27°C

Rock	S_w (DWM, %)	S_w (NMR, %)	η_o (Meas., cp)	η_o (NMR, cp)	ϕ_b	ϕ_{NMR}
1B (SS)	55	55.5	7.5	16.0	19.7	20.7
2B (SS)	12	37	7.5	8.15	18.9	20.7
3 (SS)	100	100	NA	NA	17.8	20.0
3B (SS)	50	45	7.5	8.6	17.8	20.1
4 (SS)	100	95.6	NA	250	18.5	19.3
4B (SS)	26	34	7.5	8.3	18.5	20.1
5 (LS)	100	86.7	NA	42.3	14.5	18.0
5B (LS)	28	33	7.5	11.2	14.5	18.5

the NMR total porosity is significantly higher than the buoyancy porosity for the Indiana limestone. We believe that porosity fluctuations in the sample cause the NMR porosity to read higher than the average porosity for the Indiana limestone. Differences between buoyancy porosity and NMR porosities measured on a millimeter length scale are not unexpected. Rothwell and Vinegar[20] also reported that NMR imaging porosities measured with a 1.0-mm resolution in Berea and Lion Mountain sandstone cores showed significant deviations from the average porosity. Another potential source of error in the NMR porosities determined in our experiments is likely due to our calibration procedure since the NMR porosities in Table 3 appear to be systematically higher than the buoyancy porosities. The NMR porosities were determined from the ratio of the NMR signal amplitude (at zero time) of the rock samples to that of an equal volume brine sample. The higher conductivity of the water sample probably caused the quality factor (Q) of the NMR coil to be reduced relative to the Q of the coil when the rock samples were measured. This would cause the NMR porosities to read too high. It should be noted, however, that the fluid saturations and oil viscosities in Table 3 are not affected by porosity calibration errors.

Conclusions

A new NMR method of fluid characterization has been developed, tested, and validated using Monte Carlo simulations and NMR data acquired on live and dead hydrocarbon mixtures, live and dead crude oils, and partially saturated rocks. The new method overcomes the difficulties inherent in earlier methods and represents a significant advance in NMR fluid characterization and formation evaluation.

Nomenclature

a = constitutive constant defined in Eq. 16, s·cp/K
a_l = amplitude of l-th component in brine T_2 dist., p.u.
A_g = amplitude of gas signal, p.u.
A_j^p = amplitude of j-th echo for p-th measurement, p.u.
A_{OBMF} = amplitude OBMF signal, p.u.
b = constitutive constant in Eq. 21, cm^2·cp/(K·s)
b_k = amplitude of k-th constituent in oil, p.u.
BFV = bound fluid volume (see Fig. 4), p.u.
BVI = bulk volume of irreducible water, p.u.
D_g = molecular diffusion coefficient of gas, cm^2/s
D_k = diffusion coefficient of k-th oil constituent, cm^2/s
D_{LM} = log mean of diffusion distribution in oil, cm^2/s
$D_o(\eta_k)$ = same as D_k above, cm^2/s
D_{OBMF} = molecular diffusion coefficient of OBMF, cm^2/s
D_w = molecular diffusion coefficient of brine, cm^2/s
$f(GOR)$ = empirical function defined by Eqs. 24 to 26
FFV = movable fluid volume, p.u.
f_k = proton fraction of k-th constituent in oil
G_p = applied field gradient for p-th meas., Gauss/cm

GOR = gas/oil ratio in a live hydrocarbon liquid, m^3/m^3
HI = hydrogen index
N = no. of measurements in a suite
N_o = no. of components used to fit oil T_2 relaxation
N_w = no. of components used to fit brine T_2 relaxation
N_{cut} = no. of brine T_2 components less than $T_{2,cut}$
NE_p = no. of echoes acquired for p-th measurement
P = pressure, psia
$S_{o,xo}$ = flushed zone oil saturation
S_w = water saturation in rock samples
T = temperature, K
$T_{1,g}$ = gas spin-lattice relaxation time, s
$T_{1,k}$ = spin-lattice relaxation time of k-th oil constituent, s
$T_{1,o}(\eta_k)$ = same as $T_{1,k}$ above, s
$T_{1,LM}$ = log mean of $T_{1,k}$ distribution, s
$T_{1,OBMF}$ = OBMF spin-lattice relaxation time, s
$T_{2,cut}$ = empirical bound water T_2 cutoff, ms
$T_{2,g}$ = gas diff.-free transverse relaxation time, s
$T_{2,k}$ = diff.-free relaxation time of k-th oil constituent, s
$T_{2,l}$ = bulk plus surface relaxation times of brine, s
$T_{2,LM}$ = log mean of $T_{2,k}$ distribution, s
$T_{2,o}(\eta_k)$ = same as $T_{2,k}$, s
$T_{2,OBMF}$ = OBMF diff.-free transverse relaxation time, s
TE_p = echo-spacing of p-th measurement, s
W_p = wait time
γ_H = proton (^{1}H) gyromagnetic ratio, 1/(Gauss·s)
η_k = constituent viscosity of k-th comp. in oil, cp
$(\eta_k)_{LM}$ = log mean of η_k distribution, cp
η_o = macroscopic viscosity of oil, cp
ξ = apparent T_1/T_2 ratio of brine (wetting) phase
ϕ_b = buoyancy porosity, p.u.
$\phi_{g,xo}$ = gas-filled flushed zone porosity, p.u.
ϕ_{NMR} = total NMR porosity of rock samples, p.u.
$\phi_{o,xo}$ = oil-filled flushed zone porosity, p.u.
$\phi_{OBMF,xo}$ = OBMF-filled flushed zone porosity, p.u.
ϕ_T = total porosity estimate from MRF inversion, p.u.
$\phi_{w,xo}$ = brine-filled flushed zone porosity, p.u.
$\phi_{wf,xo}$ = free-water filled flushed zone porosity, p.u.
τ_c = rotational diffusion correlation time, s
ω_0 = Larmor angular frequency, radians/s

Subscripts

g = gas
o = oil
$OBMF$ = oil-base mud filtrate
w = brine

Superscript

$\dagger$ = apparent transverse relaxation times that include bulk, diffusion, and surface (for brine) relaxation mechanisms

Acknowledgments

References

1. Akkurt, R. *et al.:* "NMR Logging of Natural Gas Reservoirs," paper N presented at the 1995 Annual Meeting of the Society of Professional Well Log Analysts, Paris, 26–29 June.
2. Prammer, M.G. *et al.:* "Lithology-Independent Gas Detection By Gradient-NMR Logging," paper SPE 30562 presented at the 1995 SPE Annual Technical Conference and Exhibition, Dallas, 22–25 October.
3. Akkurt, R. *et al.:* "Determination of Residual Oil Saturation Using Enhanced Diffusion," paper SPE 49014 presented at the 1998 SPE Annual Technical Conference and Exhibition, New Orleans, 27–30 September.
4. Looyestijn, W.J.: "Determination of Oil Saturation from Diffusion NMR Logs," paper SS presented at the 1996 Annual Meeting of the Society of Professional Well Log Analysts.
5. Slijkerman, W.F.J. *et al.:* "Processing of Multi-Acquisition NMR Data," paper SPE 56768 presented at the 1999 SPE Annual Technical Conference and Exhibition, Houston, 3–6 October.
6. Carr, H.Y. and Purcell, E.M.: "Effects of Diffusion on Free Precession in Nuclear Magnetic Resonance Experiments," *Physical Review* (1954) **94,** No. 1, 630–38.
7. Kleinberg, R. and Vinegar, H.J.: "NMR Properties of Reservoir Fluids," *The Log Analyst* (November–December 1996) 20–32.
8. Freedman, R.: "Formation Evaluation Using Magnetic Resonance Measurements," U. S. Patent No. 6,229,308 (2001).
9. Freedman, R., Heaton, N., and Flaum, M.: "Field Applications of a New Nuclear Magnetic Resonance Fluid Characterization Method," paper SPE 71713 presented at the 2001 SPE Annual Technical Conference and Exhibition, New Orleans, 30 September–3 October.
10. Morriss, C.E. *et al.:* "Field Test of an Experimental Pulsed Nuclear Magnetism Tool," paper GGG presented at the 1993 Annual Meeting of the Society of Professional Well Log Analysts, Calgary, 13–16 June.
11. Zhang, Q. *et al.:* "Some Exceptions to Default Rock and Fluid Properties," paper FF presented at the 1998 Annual Meeting of the Society of Professional Well Log Analysts, Keystone, Colorado, 26–29 May.
12. Morriss, C.E. *et al.:* "Hydrocarbon Saturation and Viscosity Estimation from NMR Logging in the Belridge Diatomite," paper C presented at the 1994 Annual Meeting of the Society of Professional Well Log Analysts, Tulsa, 19–22 June.
13. Lo, Sho-Wei: "Correlation of NMR Relaxation Time With Viscosity/Temperature, Diffusion Coefficient and Gas/Oil Ratio of Methane-Hydrocarbon Mixtures," PhD dissertation, Rice U., Houston (1999).
14. McCain, W.D.: *The Properties of Petroleum Fluids*, PennWell Publishing Co., New York City (1990) Chapter 1.
15. Forster, D.: *Hydrodynamic Fluctuations, Broken Symmetry, and Correlation Functions*, W.A. Benjamin, Inc., New York City (1975) Chapter 6.
16. Stejskal, E.O. and Tanner, J.E.: "Spin Diffusion Measurements: Spin Echoes in the Presence of a Time-Dependent Field Gradient," *J. Chem. Phys.* (1965) **42,** No. 1, 288–92.
17. Lo, Sho-Wei *et al.:* "Correlations of NMR Relaxation Time With Viscosity, Diffusivity, and Gas/Oil Ratio of Methane/Hydrocarbon Mixtures," paper SPE 63217 presented at the 2000 SPE Annual Technical Conference and Exhibition, Dallas, 1–4 October.
18. "NIST Thermophysical Properties of Hydrocarbon Mixtures Database (SUPERTRAPP)," *User's Guide,* Version 3, U.S. Dept. of Commerce (October 1999).
19. Appel, M. *et al.:* "Reservoir Fluid Study By Nuclear Magnetic Resonance," paper HH presented at the 2000 Annual Meeting of the Society of Professional Well Log Analysts, Dallas, 4–7 June.
20. Rothwell, W.P. and Vinegar, H.J.: "Petrophysical Applications of NMR Imaging," *Applied Optics* (1985) **24,** No. 23, 3969–72.

SI Metric Conversion Factors

$$
\begin{aligned}
°API \quad & 141.5/(131.5 + °API) && = g/cm \\
cp \times 1.0* \quad & E - 03 && = Pa\cdot s \\
cycles/sec \times 1.0* \quad & E + 00 && = Hz \\
ft \times 3.048* \quad & E - 01 && = m \\
°F \quad & (°F + 459.67)/1.8 && = K \\
in. \times 2.54* \quad & E + 00 && = cm
\end{aligned}
$$

*Conversion factor is exact.

Robert Freedman is the engineering adviser in the Magnetic Resonance Department at the Schlumberger Sugar Land Product Center. e-mail: freedman1@slb.com. Freedman has 26 years of experience in the oil industry, including 5 years of research and operations experience with Shell, 5 years as an independent consultant in formation evaluation, and 16 years with Schlumberger working on various engineering projects. He has made many well-known contributions to electromagnetic and NMR modeling, signal processing, and formation evaluation. Freedman holds a PhD degree in physics from the U. of California at San Diego. He has served as a technical editor for *SPEFE*. **Sho-Wei Lo** is a chemical engineer with Schlumberger in Sugar Land, Texas. e-mail: slo@sugar-land.oilfield.slb.com. She worked as a postdoctoral research associate in the chemical engineering dept. at Rice U. for six months after receiving her PhD and joined Schlumberger in June 2000. Lo holds a BA degree in chemistry and mathematics from Wheaton College and a PhD degree in chemical engineering from Rice U. **Mark Flaum** is currently pursuing a post-graduate degree at Rice U. e-mail: mflaum@rice.edu. Flaum holds a BE degree in engineering from McGill U. in Montreal, Canada. **George Hirasaki** had a 26-year career with Shell Development and Shell Oil Cos. before joining the chemical engineering faculty at Rice U. in 1993. e-mail: gjh@rice.edu. At Shell, his research areas included reservoir simulation, enhanced oil recovery, and formation evaluation. At Rice, his research interests are in NMR well logging, reservoir wettability, asphaltene deposition, emulsion coalescence, and surfactant/foam aquifer remediation. Hirasaki holds a BS degree in chemical engineering from Lamar U. and a PhD degree in chemical engineering from Rice U. He was named an Improved Oil Recovery Pioneer at the 1998 SPE/DOR IOR Symposium. **Abigail Matteson** is manager of the Petrophysical Laboratories in the Reservoir Dept. of Schlumberger-Doll Research in Ridgefield, Connecticut. e-mail: matteson@ridgefield.sdr.slb.com. Her research interests include core analysis, NMR, and mineralogy. Matteson holds BS and MS degrees in geology from the State U. of New York at Stony Brook. **Abdurrahman Sezginer** joined Sensys Instruments in 2000. e-mail: asezginer@sensys-inst.com. Sezginer joined Schlumberger-Doll Research in 1985 and contributed to the development of the CMR tool. He subsequently joined Schlumberger Sugar Land Product Center in 1997 as a project manager in the Magnetic Resonance Department. Sezginer has made many significant contributions to NMR and electromagnetic modeling, signal processing, and tool development during his employment with Schlumberger. He holds a PhD degree in electrical engineering from MIT